Environ. Sci. Technol. **1999**, *33*, 751−757

Cadmium Biosorption Rate in Protonated *Sargassum* Biomass

JINBAI YANG AND BOHUMIL VOLESKY*
Department of Chemical Engineering, McGill University, 3610 University Street, Montreal, Canada H3A 2B2

Biosorption of the heavy metal ion Cd^{2+} by protonated nonliving brown alga *Sargassum fluitans* biomass was accompanied by the release of hydrogen protons from the biomass. The uptake of cadmium and the release of proton matched each other throughout the biosorption process. The end-point titration methodology was used to maintain the constant pH 4.0 for developing the dynamic sorption rate. The sorption isotherm could be well represented by the Langmuir sorption model. A mass transfer model assuming the intraparticle diffusion in a one-dimensional thin plate as a controlling step was developed to describe the overall biosorption rate of cadmium ions in flat seaweed biomass particles. The overall biosorption mathematical model equations were solved numerically yielding the effective diffusion coefficient D_e about 3.5×10^{-6} cm^2/s. This value matches that obtained for the desorption process and is approximately half of that of the molecular diffusion coefficient for cadmium ions in aqueous solution.

Introduction

Biosorption of the nonliving brown alga *Sargassum fluitans* has been found particularly effective in binding metal ions of cadmium, one of the three most environmentally threatening toxic heavy metals. The equilibrium maximum binding capacity of the biomass for cadmium was reported to exceed 100 mg/g (dry biomass). High sorption capacity, easy regeneration, and low costs make this biomass of special interest for the purification of high volumes of low-concentration wastewater (*1*−*3*).

For any practical applications, the process design and operation control, the sorption process rate and the dynamic behavior of the system are very important factors. The dynamics of single-metal sorption in a batch system represents a suitable model system to study. Several mechanisms have been proposed to describe the rate of the biosorption process by several investigators. For example, Jang et al. (*4*) used the Shrinking Core (SC) model with single-resistance intraparticle diffusion as the controlling step to describe the biosorption of Cu^{2+} by calcium-alginate beads. Chen et al. (*5*) showed that the SC model-calculated diffusion coefficient for copper ions in a series of increasingly dense calcium alginate gel beads was not plausible. They proposed the Linear Adsorption (LA) model to describe the process of metal binding to the sorbent particles. While the effective diffusion coefficient within a matrix should be less than the molecular value, because of tortuosity and porosity of the solid phase (*6*, *7*), the LA model-calculated values of the Cu^{2+} diffusion coefficient in calcium alginate beads were greater than the molecular diffusion coefficient of Cu^{2+} in water. Apel and Torma (*8*) determined the diffusion coefficients for metal ions of Cd^{2+}, Ba^{2+}, etc. in Ca-alginate beads. The value for the Cd^{2+} diffusion coefficient reported was 1 to 2 orders of magnitude lower than the corresponding molecular value. They confirmed that the overall biosorption rate was controlled by intraparticle diffusion. However, the use of an enzyme reaction rate model, a hyperbolic rate equation, at a steady-state condition is somehow not compatible with the intraparticle diffusion controlling assumption. In our earlier work (*9*), protonated biomass of seaweed *Sargassum fluitans* was used as biosorbent to study the rate of cadmium desorption with 0.1 N HCl as elutant. An intraparticle diffusion model was proposed for the desorption process, and the effective diffusion coefficient of Cd^{2+} ions was determined in the range of 0.23−0.55 of the molecular diffusion coefficient.

The present work investigated the sorption behavior at a fixed pH 4.0. Biosorption of heavy metals by algal biomass was considered to be based on an ion exchange mechanism by Crist et al. (*10*). In the desorption process, the amount of protons bound was negligible in comparison with the concentration of the eluting acid. However, the sorption of toxic metals by protonated biomass results in the release of protons which, in turn, drives down the solution pH. Resulting significant decrease of pH from the desired value of pH 4.0 makes further sorption less favorable due to the lowered number of anionic exchange sites available. The end-point titration method was thus introduced to maintain the constant sorption pH 4.0. Since seaweed biomass particles are more like flat chips of the plant tissue rather than spherical particles, a one-dimensional plate diffusion model was proposed, and a numerical solution scheme was developed to enable the prediction of the dynamic behavior of metal ion binding.

Materials and Methods

Preparation of Sorbent. Beach-dried *Sargassum fluitans*, collected in Naples, FL, was ground in a homogenizer and sieved to different fraction sizes. The batch of biomass with particle size 1.0−1.4 mm was selected for further cross-linking and protonation processes. The cross-linking of the biomass was with formaldehyde according to Leusch et al. (*1*). To stabilize the biomass, it was necessary to eliminate the soluble component such as alginate and the light metals Ca^{2+}, Mg^{2+}, etc. in the biomass by protonating it with 0.1 N HCl (10 g biomass/L). After 3 h of contacting with acid, the biomass was rinsed with deionized water in the same volume many times until a stable wash pH 4.0 was reached. Then the biomass was dried in an oven at 40−60 °C overnight. To guarantee that different size particles of biomass were uniform in composition, the biomass particle of sizes of (0.5−0.7) mm and (0.84−1.0) mm were prepared from manually cut identical biomass parts. All biomass particles were of the same thickness of approximately 0.1 mm. Unless specified otherwise, the biomass particle size used in the latter experiments was (1.0−1.4) mm.

End-Point Titration of the Sorption Process. Following the conditioning of 0.1 g of biomass batch by mixing in 50 mL of D−H_2O (magnetically stirred vessel with baffles for about 1.0 h), the computer-driven autotitrator assembly (PHM82 pH meter, TTT80 Titrator and ABU80 AutoBuret, Radiometer, Copenhagen, Denmark) was started in the end-point titration mode set to pH 4.0. The solution pH 4.0 was controlled by the autotitrator through the addition of 0.05 N NaOH solution into the vessel by an internal high-speed pump and a buret. When the equilibrium was reached, 1.0

* Corresponding author phone: (514)398-4276; fax: (514)398-6678; e-mail: boya@chemeng.lan.mcgill.ca.

10.1021/es980412w CCC: $18.00
Published on Web 01/22/1999

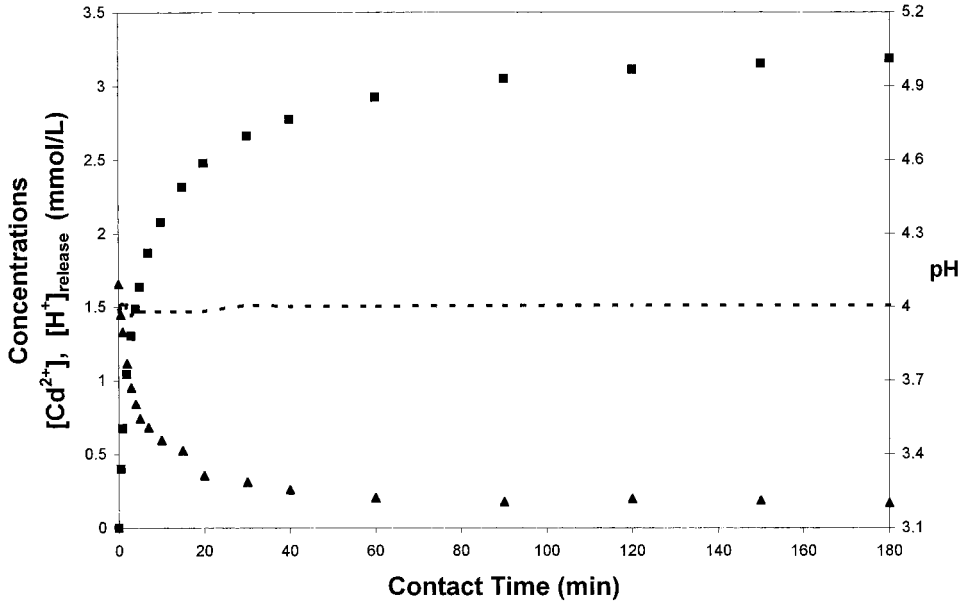

FIGURE 1. The end-point titration of cadmium biosorption with 0.05 N NaOH solution at pH 4.0. Changes during the contact time: (▲) Cd (mmol/L); (■) H^+ (mmol/L); and (—) pH.

mL of concentrated $Cd(NO_3)_2$ solution was added into the well-stirred vessel to start the metal sorption process. The initial Cd concentration was approximately 200 ppm. The pH value and the volume of the alkali added vs contacting time were recorded by the controlling computer. A series of 0.2 mL samples of solution were removed from the vessel at predefined time intervals. After appropriate dilution, the samples were analyzed for metal concentration by a flame atomic absorption spectrophotometer (AAS, Thermo Jarrel Ash, Model Smith-Hieftje II).

The metal binding was determined by the simple concentration difference method (*3*). When the initial and final metal concentrations, C_0 and C_r, respectively, were determined by AAS, the metal ion binding q was calculated from the mass balance as follows

$$q = (C_0 - C_r)\, V/W$$

where V is the solution volume and W is the mass of sorbent.

All data points in the figures presented here were the average of duplicate experimental results, and the deviations were within 5%.

Experimental Results

Speciation in Solution. While there was no hydrolysis of cadmium ions in solution at pH 7.0 or lower, according to the computer program MINEQL+ (*11*), almost all the cadmium was present in the free ion form, i.e., Cd^{2+} at the experimental pH 4.0. As a consequence, the consumption or release of protons due to water hydrolysis in the aqueous solution phase was negligible. No precipitation was observed in the experimental process as predicted by the program.

Response of pH Probe in Titration. Since the autotitrator assembly can read pH value in the solution as fast as 1−8 times every second and the pumping speed of the internal autoburet is fast and adjustable up to 0.1 mL/s, the protons released from the biomass caused by the sorption of Cd cations could be neutralized almost instantly by adding NaOH solution into the reactor. The pH value of the solution was thus maintained at a constant level, pH 4.0 in this case. The pH fluctuated only within a very narrow range of pH 3.95−4.05. In Figure 1, the change of pH value, Cd concentration and H^+ release were plotted against the sorption contact time. The proton release was calculated from the consumption of the NaOH added to the sorption system for maintaining the constant pH 4.0.

Sorption Rate. The biosorption rate of the Cd cation onto the (1.0−1.4) mm size biomass particles is shown in Figure 2. The rate of the proton released reflected the cadmium ion uptake rate well throughout the process. The sorption rate appeared to go through two stages. The first stage was fast and about 75% of the total cadmium adsorption took place in 15 min. The second stage was relatively slower, and it took approximately 3 h to reach the sorption equilibrium. Furthermore, using the first-order rate method used for biosorption by Crist et al. (*12*), the sorption rate was assumed proportional to the binding capacity in the biomass, i.e., $d[H]/dt = k([H]_m - [H])$ where t is the contact time, k is the rate constant, and $[H]$ and $[H]_m$ stands for the instant and maximum proton release, respectively. The integrated form of the first-order rate equation, $\ln([H]_m - [H]) = kt$, was plotted in Figure 2A. The different slopes of lines represent the sorption rate constants, more clearly demonstrating the fast and slow process periods. Similar results, not shown here, were obtained for other sizes of biomass particles.

The Effect of Biosorbent Particle Size on the Cd Sorption Rate. External and internal mass transfer resistance by the biomass particle are of concern for the sorption dynamics. The effect of agitation speed on the biosorption rate was examined first. A series of sorption experiments was carried out at different agitation rates. After the agitation rate increased beyond a critical degree, the resulting time profiles of the Cd ion concentration in the bulk solution did not change further and agreed with each other within about 5% error (not shown). In further approach, the experimental agitation rate was set at 3 Hz (above the critical rate) so that the effect of the fluid mass transfer resistance became negligible under the experimental conditions.

The effect of the biosorbent particle size was investigated in a similar way. The time profiles of the dimensionless Cd concentration were compared for different sizes of *Sargassum* biosorbent particles as shown in Figure 3. The solid curve is the model prediction (described later) and the scattered points are from the experiments. The concentration profiles for three different particle sizes of (0.5−0.7) mm, (0.84−1.00) mm, and (1.0−1.4) mm agreed with each other within the deviation of about 5%. This indicates that the overall sorption

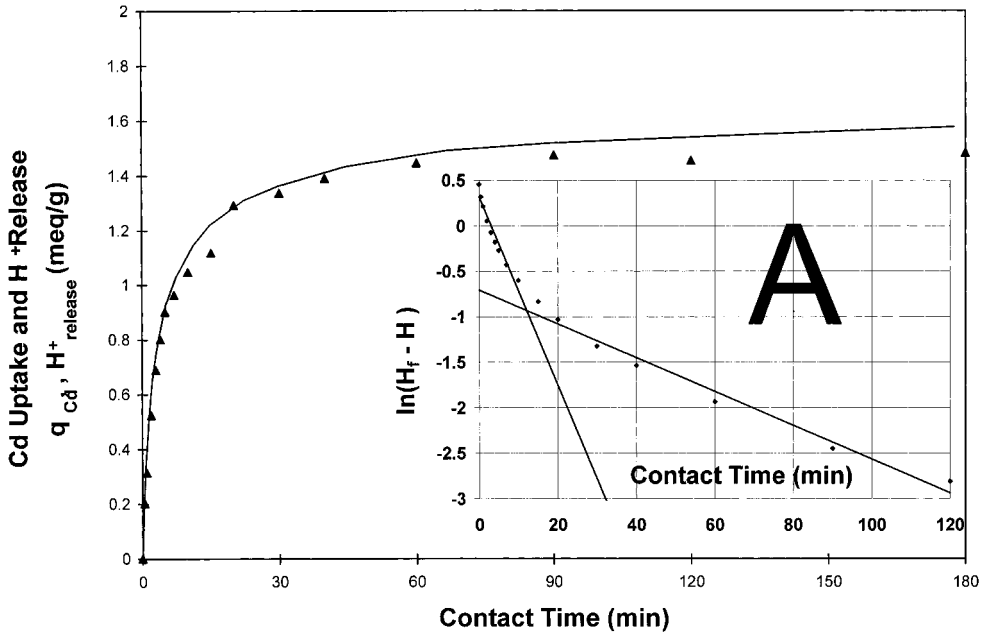

FIGURE 2. Dynamics of the cadmium metal uptake and proton release in time at pH 4.0: (—) $H^{+}_{release}$ (meq/g) and (▲) q_{Cd} (meq/g). (2A) Slopes of the first-order rate equation (ln $C = kt$) indicate reaction rates.

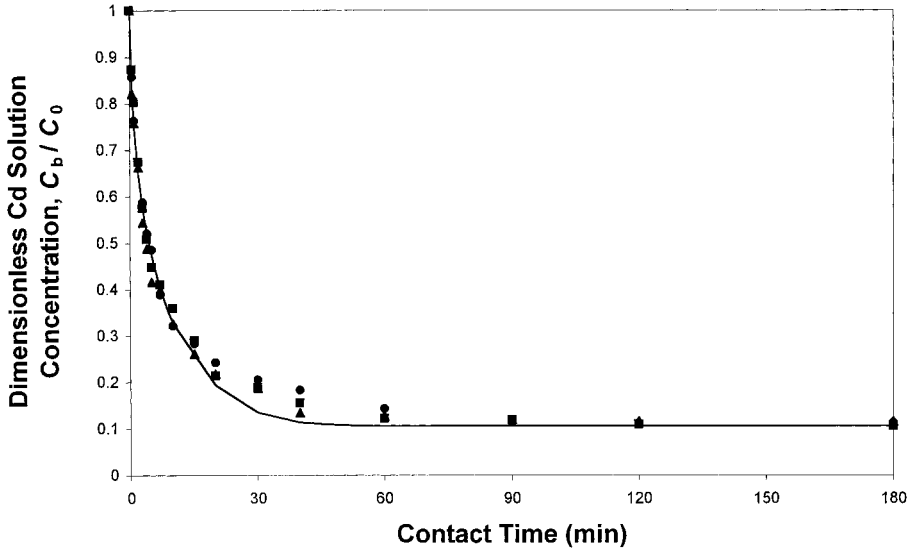

FIGURE 3. The equilibrium cadmium concentration in solution decreased with contact time for different biomass particle sizes: (●) particle 1: (0.5−0.7) mm; (▲) particle 2: (0.84−1.0) mm; (■) particle 3: (1.0−1.4) mm; (—) model.

rate of Cd on the biomass is independent of the biosorbent particle size used.

The *Sargassum* biomass was reinforced by formaldehyde cross-linking. The sorption rate for the cross-linked biomass particle size of (1.0−1.4) mm, detected by a similar experimental procedure, was lower than that for native biomass (Figure 4).

Mathematical Model. For quantitative description of the biosorption process dynamics it is necessary to develop a mathematical model capable of reflecting the toxic metal ions concentration change with the contact time. Generally, biosorption of metal ions consists of three continuous processes. The metal ions first diffuse across the particle-to-fluid film from the bulk solution before they enter the biosorbent. Then they diffuse further toward the binding sites through the gel phase of the biomass material. Finally, the metal ions react with the chemical groups of the binding sites. In our earlier work on cadmium desorption, the intraparticle diffusion of Cd ions was assumed as the rate controlling step (*9*). For the sorption process, similar assumptions are made here as follows:

The particle-to-liquid mass transfer resistance has been eliminated through adequate turbulence created by proper agitation.

The sorption reaction between the Cd cation and binding sites on the biomass is much faster than diffusion of the Cd cation inside the biomass material, i.e., the overall sorption rate is controlled by the intraparticle diffusion.

For the relatively flat seaweed *Sargassum* biomass particle, the thickness of the particle is much smaller than the length and width. Thus the biomass particle can be considered as a thin plate. The intraparticle diffusion along one dimension, i.e., the thickwise direction, controls the diffusion rate of the overall process.

The amount of adsorbed metal ions inside the biomass particle is in equilibrium with the metal concentration in the liquid phase and the Langmuir sorption isotherm relationship holds

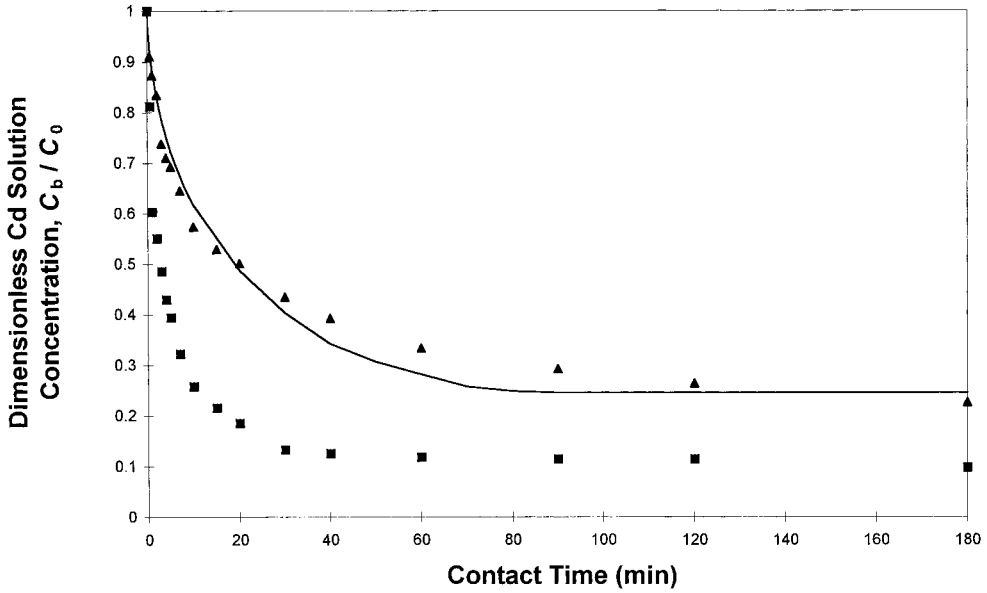

FIGURE 4. Cadmium concentration decrease with contact time for cross-linked biomass and not cross-linked biomass: (■) native biomass (experimental); (▲) cross-linked biomass (experimental); and (—) cross-linked biomass (model).

$$q = \frac{q_m C_r}{K + C_r} \tag{1}$$

where q is the uptake of metal on the biomass, C_r is the final equilibrium concentration of the metal in the liquid phase, q_m is maximum metal uptake, and K is the Langmuir equilibrium constant.

It should be indicated that the Langmuir adsorption assumptions did not reflect the experimental results which demonstrated a proton release as a result of ion exchange with metal ions. Thus the diffusion of metal ions into the biomass must accompany the protons diffusing out into the bulk liquid. However, the diffusion coefficient of H^+ is several times higher than that of Cd^{2+} ions in infinitely diluted aqueous solutions (*13*, *14*) which is a reasonable assumption for the present system studied. In addition, Crist et al. (*15*) show that the Langmuir model could be used for ion exchange rate calculations for algal biomass in a certain concentration range. It is thus reasonable to assume that the overall sorption rate was just controlled by the movement of Cd^{2+} ions.

The electroneutrality in the solution was maintained by the existence of co-ions, NO_3^- in this case. Both HNO_3 and $Cd(NO_3)_2$ are strong electrolytes which were dissociated into counterions and co-ions in the aqueous solution. The transport of counterions was accompanied by the co-ions in the form of ion pairs. Thus the faster diffusion of protons did not necessarily destroy the electroneutrality. Instead, the overall diffusion rate was controlled by the slower diffusing Cd ions, which was governed by the Fick's Law.

Strictly speaking, the *Sargassum* seaweed material should perhaps be considered as a heterogeneous material. The calculation of the diffusion coefficient would then require a good knowledge of the material such as porosity, etc. However, because of the biological nature of the gel-like seaweed material it could be considered as a quasi-homogeneous phase for the mathematical treatment (*6*, *16*). The effect of the crystal ratio (close to the unity) was thus lumped into the effective diffusion coefficient. It has to be realized that for some systems the existence of the porosity is the main difference between the effective and the true value of the diffusion coefficient. When the porosity is close to one, the main difference is caused by the tortuosity within the porous network.

Based on the model assumptions, the mass conservation equations for metal ions in the biomass particle and bulk solution are as follows

$$\frac{\partial C_r}{\partial t} + \rho \frac{\partial q}{\partial t} = D_e \frac{\partial^2 C_r}{\partial r^2} \tag{2}$$

$$V \frac{dC_b}{dt} = -D_e S_t \frac{\partial C_r}{\partial r}\Big|_{r=R} \tag{3}$$

where r is the arbitrary position coordinate from the central line of the biomass particle in the thickwise direction, and t is the time elapsed from the start of the sorption process. C_b and C_r represent the metal concentrations in the bulk solution and in the biomass gel phase at layer r inside the biomass, respectively. R is the half-thickness of the biomass particle, ρ is the density of the biomass, V is the volume of bulk solution, and S_t is the total surface area of particles. D_e represents the effective intraparticle diffusion coefficient.

The boundary and initial conditions for the sorption process are as follows:

$$C_r|_{r=R} = C_b \qquad (r = R,\ t > 0) \tag{4}$$

$$\frac{\partial C_r}{\partial r}\Big|_{r=0} = 0 \qquad (r = 0,\ t > 0) \tag{5}$$

$$C_b = C_0 \qquad (t = 0) \tag{6}$$

$$C_r = 0 \qquad (t = 0,\ 0 \le r < R) \tag{7}$$

where C_0 is the initial metal concentration in the solution.

Differentiating the isotherm eq 1, we obtain

$$\frac{\partial q}{\partial C_r} = \frac{K q_m}{(K + C_r)^2} \tag{8}$$

Introducing dimensionless variables $x = r/R$, $C(x,t) = C_r/C_0$, $\bar{C}(t) = C_b/C_0$, substituting eq 8 into the rate eq 2 and rewriting eq 3 leads to the following coupled equations

$$f(C)\frac{\partial C}{\partial t} = \alpha \frac{\partial^2 C}{\partial x^2} \tag{9}$$

$$\beta \frac{d\bar{C}}{dt} = -\alpha \frac{\partial C}{\partial x}\Big|_{x=1} \tag{10}$$

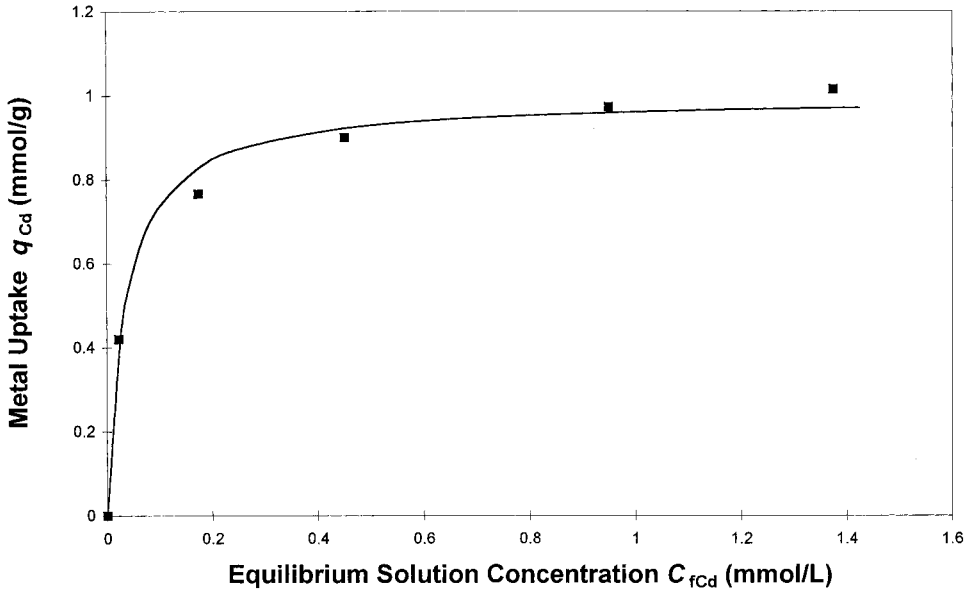

FIGURE 5. Cadmium sorption isotherm experimental data and Langmuir model regression: (■) experimental and (—) Langmuir model: q_m = 0.994 mmol/g, K = 0.035 mmol/L.

where $f(C)$ is defined as a nonlinear function of the dimensionless concentration C:

$$f(C) = \left(1 + \frac{\gamma_1\gamma_2}{(C+\gamma_1)^2}\right) \tag{11}$$

$\beta = V/S_tR$, $\gamma_1 = K/C_0$, and $\gamma_2 = \rho q_m/C_0$ are auxiliary dimensionless parameters, while $\alpha = D_e/R^2$ has units of s^{-1}.

The corresponding boundary and initial conditions are as follows:

$$C(1,t) = \bar{C}(t) \qquad (x = 1,\ t > 0) \tag{12}$$

$$\frac{\partial C}{\partial x}|_{x=0} = 0 \qquad (x = 0,\ t > 0) \tag{13}$$

$$\bar{C}(0) = 1 \qquad (t = 0) \tag{14}$$

$$C(x,0) = 0 \qquad (t = 0,\ 0 \le x < 1) \tag{15}$$

Equations 9 and 10 are simultaneous nonlinear partial differential equations (PDEs) with respect to C and $\bar{C}$, respectively. They are similar to the ones used in diffusion of a gas in microvoids of a polymer. For linear isotherms, an analytical solution was presented by Crank (*17*). In the case of nonlinear isotherms, such as Langmuir isotherm used in eq 1, the analytical solution is not available, and a numerical method must be applied to solve the complicated equations. In this work, the Galerkin Finite Element Method (GFEM) (*18*) was applied to discretize the model PDEs, leading to a series of ordinary differential equations (ODEs). The Euler backward integration in time was applied to obtain the numerical solution for dimensionless intraparticle concentration $C(x, t)$ and dimensionless bulk concentration $\bar{C}(t)$.

Among the model parameters, K and q_m could be obtained from batch equilibrium experiments. R (0.005 cm) and ρ (1050 g/1000 cm^3) could be measured directly and total surface area of biomass particle, S_t (57.14 cm^2) is decided by the weight of the biomass used W (0.3 g wet) and the thin plate geometry of the biomass particle. All other parameters, except D_e, could be calculated once the volume V (0.05 L) and the concentration of the metal solution in the reactor are specified. This means that the numerical solution of the model equations is uniquely determined by the value of D_e. In other words, a specific value of D_e is corresponding to a specific simulated concentration profile of the $\bar{C}(t)$ vs t curve. The intraparticle diffusion coefficient D_e could thus be regressed from the comparison of the simulated profile curves and the experimental results by minimizing the following objective function

$$\varphi = \sum_{i=1}^{N} |(\bar{C}_{model} - \bar{C}_{experimental})/\bar{C}_{experimental}|_i \tag{16}$$

where i is the ith experimental data point and N is the total number of experimental data points. A computer program was developed to facilitate all the above calculation procedures. The lack of analytical solution also means that uncertainty analysis is difficult to derive as well. The current practice to obtain an estimate of uncertainty in this case is to perform a sensitivity analysis on the fitted parameter D_e. While various methods exist to do so, the sensitivity analysis was not considered relevant within the framework of this work.

Equilibrium biosorption experiments were conducted at pH 4.0, and the result is shown in Figure 5. The Cd uptake was plotted against the final concentration of Cd in the bulk solution. The solid curve was regressed from the scattered experimental data with Langmuir model (eq 1) using K = 0.035 mmol/L and q_m = 0.994 mmol/g.

As in Figure 3, the model-simulated concentration profile curve was plotted as a solid line. The corresponding D_e value of 3.5×10^{-6} cm^2/s, which is an average for multiple experiments, was regressed from the corresponding experimental data. In Figure 6, a model predicted titration volume of the added alkali solution and the actual titration volume recorded by the controlling computer were plotted against the contact time. The fact that the simulation curve and the experimental data points are in an agreement within about 10% average deviation demonstrates that the model can describe the experimental data with an acceptable accuracy. The 10% average deviation is somewhat high for curve fitting. The data points in the transient range between the fast adsorption stage and the slow one contribute most to the deviation. In this range, the metal concentration in the bulk liquid was decreased to a low level whereby a small deviation, therefore, could cause a large relative error. The fact that the seaweed biomass is a natural material with a very complex composition may also be responsible for reducing the accuracy of the model prediction.

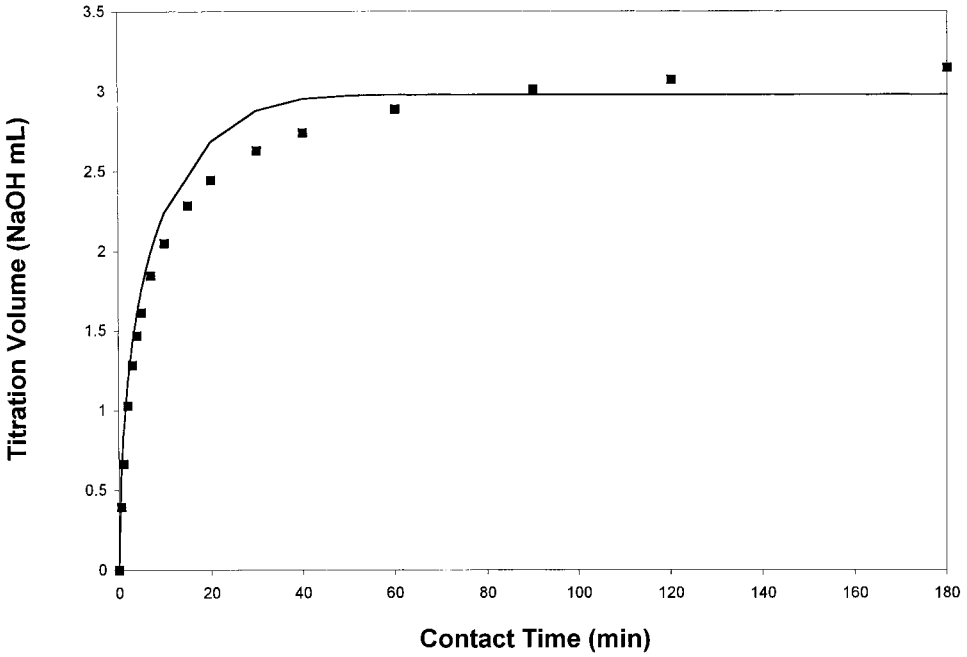

FIGURE 6. Comparison of experimental titration volume time profiles and model-predicted numerical simulation results. NaOH concentration 0.05 N: (■) experimental and (—) model.

Discussion

The Metal Uptake and the Proton Release Rate. Biosorption of Cd took place very fast during the initial stage of contact (Figure 2). It was physically difficult to sample the reaction solution at the early stage of the sorption process which has a significant effect on the overall sorption rate. This was a serious limitation to the accuracy of the data regression process used for determining the diffusion coefficient. The agreement between the cadmium metal uptake and the proton release during the sorption process indicates an equivalent ion exchange between Cd^{2+} and H^{+}. With a fast pH probe response and titration speed, the computer-recorded titration volume of the NaOH vs contact time (up to eight points per second) a correlation could be used to regress the effective diffusion coefficient directly. This method provides a useful alternative to the fast evaluation of the sorption rate, avoiding the tedious procedure of reactor solution sampling for metal concentration determination.

As indicated in Figures 2 and 2A, the sorption rate could be divided into two stages, the fast initial rate followed by a much slower sorption rate. This has often been reported by other researchers. Crist et al. (*12*)observed a similar phenomenon for the Ca ions replacing protons on peat moss biosorbent. Brassard et al. (*19*) attributed the fast initial metal sorption rate to the surface binding by natural particles and the following slower sorption to the interior penetration. In the case of *Sargassum* seaweed particles, the active binding groups reside in the cell wall and due to its large surface the initial sorption rate is accelerated. The actual mechanism of Cd sequestration has been studied only to a limited extent (*20*) and should be studied further.

Effect of Particle Size on the Sorption Rate. The experimental results indicated that the particle size does not affect the sorption rate. While this seems to be contradictory to the general idea of intraparticle diffusion controlling the process, it is necessary to point out that the grinding of biomass and particle size grading by standard sieves only work on the length and width dimensions. All sizes of the *Sargassum* biomass chip-like particles are actually of the same thickness which determines the diffusion distance. This is reflected in the present model which assumed a one-dimensional thin plate as the intraparticle diffusion field. A special care was taken in producing the biomass particles. The structure of the seaweed biomass is not homogeneous, and different parts of the seaweed offer different resistance to grinding. Thus different sizes of the sieved biomass may differ in composition resulting in a dependence of the sorption rate on the particle size.

Evaluation of the Diffusion Coefficient. In general, the diffusion process inside a porous material is slower than that in a corresponding homogeneous system having the same liquid composition as in the pore phase (*6*, *7*). In the brown alga *Sargassum* biomass, alginate is the main component responsible for the metal sorption (*21*). It is present in a gel form in the cell wall which appears very porous and easily permeable to small ionic species (*22*, *23*). The actual mobility of the diffusing entity in the dense-phase gel may be somewhat reduced by mechanical friction or interaction with the cell wall molecules. As a result, the calculated intraparticle diffusion coefficient is an effective diffusion coefficient, i.e., D_e, and it is usually smaller than the molecular diffusion coefficient D_m considered in the absence of the sorbent material matrix. For Cd^{2+}, D_m was assessed as 7.19×10^{-6} cm^2/s (*13*, *14*) and the D_e/D_m calculated with the presently regressed value was 0.486 which is in a good agreement with the one determined for the desorption process (*9*). A smaller D_e/D_m ratio of 0.14, calculated from the results in Figure 4 for cross-linked biomass, correctly reflects the retarding effect of cross-linking of the sorbent framework on the sorption rate.

In summary, the end-point titration method is suitable for the determination of sorption rate at a constant pH value. The rate of Cd^{2+} biosorption on *Sargassum fluitans* biomass could be described properly by a simple one-dimensional intraparticle diffusion model. The diffusion coefficient of Cd^{2+} ion in the biomass regressed from the model at pH 4.0 was about 3.5×10^{-6} cm^2/s, this being approximately half of the corresponding molecular diffusion coefficient value.

Glossary

C	dimensionless Cd concentration inside the particle
$\bar{C}$	dimensionless Cd concentration in bulk solution

C_0	initial Cd concentration in bulk solution (mg/L)
C_b	*Cd* concentration in bulk solution at time *t* (mg/L)
C_r	Cd concentration in the biomass gel phase at position *r* and time *t* (mg/L)
D_e	effective intraparticle diffusion coefficient (cm^2/s)
D_m	molecular diffusion coefficient (cm^2/s)
$[H]$, $[H]_m$	the instant and maximum proton release, respectively (meq/g)
K	Langmuir equilibrium constant (mg/L)
k	the first-order biosorption rate constant (L/meq)
q_m	Langmuir maximum uptake (mg/g)
q	uptake (mg/g)
r	arbitrary position coordinate (cm)
R	half thickness of the biomass particle (cm)
S_t	total surface area of biomass particles (cm^2)
t	time (s)
V	solution volume (L)
W	biomass weight (g)
x	dimensionless arbitrary position coordinate (cm)
α	D_e/R^2, (s^{-1})
β	$V/(S_t R)$, (dimensionless)
γ_1	K/C_0, (dimensionless)
γ_2	$\rho q_m/C_0$, (dimensionless)
ρ	density of biomass g/(1000 cm^3)
φ	objective function for curve fitting (dimensionless)

Literature Cited

(1) *1*) Leusch, A.; Holan, Z. R.; Volesky, B. *J. Chem. Technol. Biotechnol.* **1995**, *62*, 279−288.
(2) Aldor, I.; Fourest, E.; Volesky, B. *Can. J. Chem. Eng.* **1995**, *73*, 3, 516−522.
(3) Volesky, B.; Holan, Z. R. *Biotechnol. Prog.* **1995**, *11*, 235−250.
(4) Jang, L. K.; Brand, W.; Resong, M.; Mainieri, W.; Geesey, G. G. *Environ. Prog.* **1990**, *9*, 269−274.
(5) Chen, D.; Lewandowski, Z.; Roe, F.; Surapaneni, P. *Biotechnol. Bioeng.* **1993**, *41*, 755−760.
(6) Helfferich, F. *Ion Exchange*; McGraw-Hill: New York, 1962; pp 299−319.
(7) Westrin, B.; Axelsson, A. *Biotechnol. Bioeng.* **1991**, *38*, 439−446.
(8) Apel, M. L.; Torma, A. E. *Can. J. Chem. Eng.* **1993**, *71*, 652−656.
(9) Yang, J.; Volesky, B. *J. Chem. Technol. Biotechnol.* **1996**, *66*, 355−364.
(10) Crist, R. H.; Martin, J. R.; Guptill, P. W.; Eslinger, J. M.; Crist, D. R. *Environ. Sci. Technol.* **1990**, *24*, 337−342.
(11) Schecher, W. D. *MINEQL+: A Chemical Equilibrium Program for Personal Computers, Users Manual Version 2.22*; Environmental Research Software, Inc.: Hallowell, ME, 1991,
(12) Crist, R. H.; Martin, J. R.; Chonko, J.; Crist, D. R. *Environ. Sci. Technol.* **1996**, *30*, 2456−2461.
(13) Horvath, A. L. *Handbook of Aqueous Electrolyte Solutions*; Ellis Horwood: West Sussex, U.K., 1985; p 289.
(14) Dobos, D. *A Handbook for Electrochemists in Industry and Universities*; Elsevier Scientific: Amsterdam, The Netherlands, 1994; p 88.
(15) Crist, R. H.; Martin, J. R.; Carr, D.; Watson, J. R.; Clarke, H. J.; Crist, D. R. *Environ. Sci. Technol.* **1994**, *28*, 1859−1866.
(16) Holl, W.; Sontheimer, H. *Chem. Eng. Sci.* **1977**, *32*, 755−762.
(17) Crank, J. *Mathematics of Diffusion*, 2nd ed.; Clarendon Press: London, U.K., 1975; p 94.
(18) Lapidus, L.; Pinder, G. E. *Numerical Solution of Partial Differential Equations in Science and Engineering*; Wiley: New York, 1982.
(19) Brassard, P.; Macedo, E.; Fish, S. *Environ. Sci. Technol.* **1996**, *30*, 3216−3222.
(20) Crist, R. H.; Oberholser, K.; Schwartz, D.; Marzoff, J.; Ryder, D.; Crist, D. R. *Environ. Sci. Technol.* **1988**, *22*, 755−760.
(21) Fourest, E.; Volesky, B. *Appl Biochem Biotechnol* **1997**, *67*, 33−44.
(22) Percival, E.; McDowell, R. H. *Chemistry and Enzymology of Marine Algal Polysaccharides*; Academic Press: London, U.K., 1967; pp 99−126.
(23) Dodge, J. D. *The Fine Structure of Algal Cells*; Academic Press: London, U.K., 1973; pp 14−45.

Received for review April 21, 1998. Revised manuscript received September 24, 1998. Accepted November 2, 1998.

ES980412W